SIMULATION AND PERFORMANCE PREDICTION FOR THE RADIATION PATTERNS OF FEW-MODED AND MULTI-MODED CORRUGATED HORNS

T. Peacocke, J.A. Murphy
Experimental Physics, National Univ. of Ireland Maynooth, Co. Kildare, Ireland
Tully.Peacocke@nuim.ie, Anthony.Murphy@nuim.ie

***Abstract*—Corrugated horn assemblies are the most common method of feeding bolometer cavities for power detection on CMB experiments. Traditionally these have been single moded, whether polarised or unpolarised, but if polarisation is not required greater throughput can be obtained from few-moded or multi-moded horns. The simulation of these assemblies is far more computationally intensive than for single moded systems, and the effort is often compounded by the design of the assemblies. Here we show that multi-moded horn assemblies can be modelled reliably and do perform as required, but performance prediction requires attention to manufacturing tolerances as well as the system design.**

I. Introduction

The numerical simulation of corrugated horns by the method of mode matching has been in common use at least since an outline of the method, as applied to single moded horns and waveguides, was published in [1] building upon earlier work in [2]. The same methodology was developed at NUI Maynooth for the analysis of multi-moded horns, and mode matching code written and applied to the design of both single and multi-moded horns for CMB applications, in particular for Planck [3] and QUaD [4]. Recently we have become interested in the problem of reliably and efficiently simulating corrugated and smooth walled bolometer feed assemblies built up from horn, waveguide, filter, and other sections, and the effects of manufacturing tolerances upon performance; particularly for few-moded and multi-moded CMB applications. These assemblies can have thousands of scattering junctions. Furthermore, if two horns face each other and are coupled through a free-space or filter section, perhaps via a lens assembly, they form a leaky cavity-like component and accurate modelling of the radiation pattern of the assembly is strongly influenced by the ability to represent the electromagnetic field structure within these cavity-like sections (see Fig. 2). Configurations of this type are fairly common in both CMB instruments (Planck [3], Arceops [5], BICEP [6]) and laboratory experiments, and recent simulations and measurement show that the transmission of the entire assembly and the modal structure of the field in the radiating aperture varies rapidly with frequency and is strongly influenced by manufacturing tolerances. High frequency multi-moded horns usually operate over wide bands; this, and the sensitivity to manufacturing tolerances means that reliable beam pattern prediction becomes a significant computational challenge.

In this paper we are concerned with the general power transmission performance of these horn assemblies, their sensitivity to manufacturing tolerances, and the possibility of obtaining essentially identical performance by replacing the cavity-like assembly with smooth walled equivalents.

Section II briefly describes the method of mode matching and the approach we have taken to its numerical implementation. Section III describes efficient simulation of the structures at the design and analysis phase and section IV addresses the effects of manufacturing tolerances and the problems for performance prediction that result. We address the problem of reliability of the method and the interpretation of numerical predictions. In section V we present a comparison between measurements and simulations of a complex, multi-moded, corrugated horn assembly and in section VI our conclusions are summarised.

II. Mode Matching and Numerical Implementation

The scattering of electromagnetic radiation within a corrugated structure, or within a tapering smooth walled structure approximated by steps, is described by an operator between two Hilbert spaces. Here we are interested in the case of a horn of circular cross section under the assumption of perfect conductivity, though the method is applicable to any cross-section. In each section of the horn the field can be expanded in terms of the transverse electric and magnetic waveguide modes: complex functions on the disc with radial dependence described by Bessel functions of the first kind and integer order and angular dependence given by classical Fourier series. The transverse field in the waveguide is a Fourier-Bessel expansion of the field strength vectors in terms of these triply indexed basis functions, the 'modes'. If $\mathcal{H}_L$ and $\mathcal{H}_R$ are the spaces of fields to the left and right of a scattering junction, then the scattering is described by an automorphism of $\mathcal{H}_L \oplus \mathcal{H}_R$. Each of $\mathcal{H}_L$ and $\mathcal{H}_R$ decompose into a direct sum of subspaces $\mathcal{E} \oplus \mathcal{H}$ spanned respectively by orthonormal bases of transverse electric, TE, and transverse magnetic,

TM, modes. Orthogonality of the mode functions on the disc decomposes each of these spaces into an infinite direct sum indexed by azimuthal order, thus decomposing the fields and the scattering operators into azimuthal orders. Each azimuthal order can then be treated independently. This assumes perfect concentricity of all sections, a reasonable assumption for all practical purposes. Details of the theory are given in [1] and [7]; here we sketch an outline. The total transverse electric field in each azimuthal order on either side of the junction must match, as must the total transverse magnetic fields. Scattering is determined by enforcing conservation of total power across the junction and are given by integrals of the type

$$(\alpha_\nu - \beta_\nu) \int_A \left(\mathbf{e}_\mu^L \times \bar{\mathbf{h}}_\nu^L \right) \cdot \, \mathrm{d}A = (\gamma_\kappa - \delta_\kappa) \int_A \left(\mathbf{e}_\mu^L \times \bar{\mathbf{h}}_\kappa^R \right) \cdot \, \mathrm{d}A$$

$$(\alpha_\nu + \beta_\nu) \int_A \left(\mathbf{e}_\mu^L \times \bar{\mathbf{h}}_\kappa^R \right) \cdot \, \mathrm{d}A = (\gamma_\kappa + \delta_\kappa) \int_A \left(\mathbf{e}_\nu^L \times \bar{\mathbf{h}}_\kappa^R \right) \cdot \, \mathrm{d}A$$

for appropriate complex coefficients α_ν, β_κ, γ_μ and δ_ν. For circular apertures, A, the integrals reduce to Lommel integrals.

The scattering operators at the individual junctions, J_k^n, combined with phase slippage along adjacent sections (which are described by a diagonal operator with entries determined by the wavenumber in the guide section and the mode indices) give operators S_k^n. Let S^n denote the operator that describes the scattering of fields of azimuthal order n for the entire assembly; it is given by an associative product over all sections: $S^n = S_m^n \circ \cdots \circ S_1^n$. The domain of S_1^n is the input to the system, the codomain of each S_k^n is the domain of S_{k+1}^n, and the codomain of S_m^n is the radiating aperture of the horn. We model the illumination of the assembly by a grey or black body representing a bolometer cavity, or as an operator matrix describing the coupled modal structure of the field in the bolometer cavity/waveguide transitions, if it is know.

Regard the fields as represented in the operator space. Assume for simplicity that the source is a perfect black body. On input all modes are given unit power and the field is represented by the identity operator. This scatters with S_1^n giving a new field/operator which then scatters with S_2^n, and so on. Associativity of the product allows the computation of the scattering by the entire assembly to be broken down for computation into convenient sections, exploiting any repetition of components to reduce the total amount of computation involved.

For numerical work the infinite dimensional complex Hilbert spaces are replaced by finite dimensioned ones and the operators become ordinary complex matrices. The immediate consequence of this reduction in dimension is an approximation to the initial idealisation: at every junction every modal component of the field of every azimuthal order scatters into an infinite set of modes of the same azimuthal order and truncating the model means detail and power is lost. In an adequate model the only loss is of information

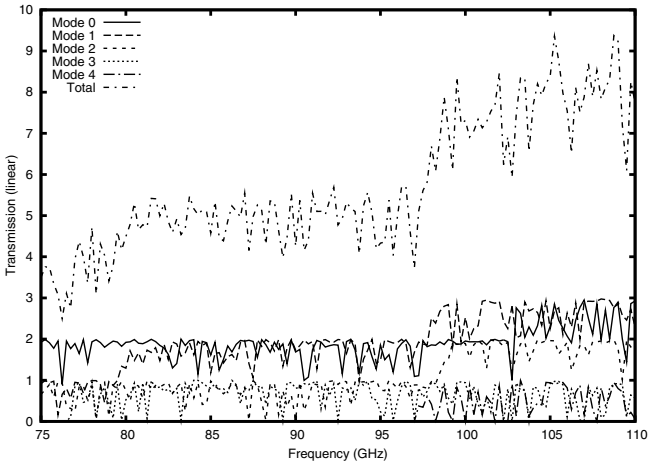

Fig. 1: Total (top curve) and per-mode power transmission (linear scale) through the assembly in Fig.1.

described by the scattering amplitudes into and out of high order evanescent field components. Nevertheless, when, as here, there are cavity-like sections in the assembly there is a lot of power in evanescent modes and much scattering takes place between the evanescent and the propagating modes. To reliably model assemblies of the type under discussion much larger numbers of modes must be included in the model than is required to model the radiation pattern from a horn coupled directly to a bolometer cavity. It is this which makes the modelling of such systems numerically intensive.

Although it can be necessary to include a large number of modes within each azimuthal order in the matrix model of the system, the number of azimuthal orders that propagate through the entire system is usually low and the orthogonal complement of the kernel of the system operator, $S = \bigoplus S^n$, is generally of low, frequency dependent dimension, and spanned by a set of coherent field vectors contributing independently to the field pattern of the horn. In the examples considered here the azimuthal orders that propagate through the entire assembly is typically orders 0 through to 4 and the dimension of the space spanned by the coherent radiated fields is between 6 and 20. All these numbers are system and frequency dependent in multi-moded horns. The model describing the system is set of system matrices S at each frequency. The final step in the modelling process is to find, form each S, the minimal spanning set of coherent fields that describes the aperture field. The components of these vectors determines the throughput and the beam pattern of the system at this frequency and is related to the Frobenius norm of S.

The equations used to determine the scattering coefficients in the S_k^n are to be found in [1], [3] and [7]. For efficient and reliable numerical implementation we exploit the structure of the matrices in a PLU factorisation (see [8]) and the stability of the scattering model checked and the reliability assessed at every junction and scattering product $S_k^n \circ S_{k+1}^n$ by checking the reciprocal condition number and pivot growth factor, and by forcing conditions on the minimal number of evanescent modes. The number of modes to be used in the model to

ensure convergence is a delicate issue for systems of the type we consider here. Increasing the number of modes changes the dimension of the underlying complex model space and the total input power. To avoid the use of extremely large and computationally intensive models a compromise has to be struck. The models are most sensitive in the regions where modes are cutting on, and a suitable measure of convergence is the total radiated power over several sample frequencies spanning each of the cut-on regions separately.

Figure 1 illustrates the variation in the total transmitted power and the total transmitted power per azimuthal order as a function of frequency in the W band system illustrated in Fig. 2.

III. Application to System Design

At the design phase maximum advantage can be taken of the algebraic formalism of mode matching. The system is perfect in the sense that section radii and lengths are known without error. If the system has two or more identical sections, possibly reversed such as two identical horns facing each other, then associativity of the scattering product means that it is only necessary to determine the scattering operator for that section once, with reversal of the system amounting to a permutation of the component's S-matrix.

Consider the system illustrated in Fig. 2; it is described by a product of operators of the following type:

$$S = T_4 \circ W_4 \circ T_3 \circ W_3 \circ T_2^R \circ W_2 \circ F \circ W_2 \circ T_2 \circ W_1 \circ T_1. \quad (1)$$

Here W is a section of waveguide, T any tapered section or section of varying radius, and F a filter, free space or lens section. T_2^R means the component is identical to T_2, but reversed. The operator H is to be read with T_1 corresponding to the short input (profiled) taper section at the left hand side of Fig. 2 where the horn joins the bolometer cavity, and so on through to the radiating aperture on the output side of the flare, T_4, at the left side of the figure. This is quite a common construction and is similar in construction to the Planck horns [9]. The input to the system is to T_1, and the output from T_4. We take advantage of the symmetries in the scattering operators: within the waveguide sections the symmetry across pairs of junctions is exploited to reduce the determination of W to the calculation of powers of a single symmetric waveguide-junction-waveguide-junction-waveguide operator. In a waveguide section the scattering matrix has sub-matrix components $S_{21} = S_{12}$ and $S_{11} = S_{22}$. The work done in calculating the matrix and in forming the scattering product powers of such matrices is thereby halved. It is immediate that the codomain of T_2^R is the same as the domain of T_2, and therefore W_1 and W_3 are powers of the same symmetric operator. Exploitation of such symmetries can greatly reduce the overall computational burden in the analysis of the system. When simulating manufacturing tolerances as outlined in section IV these symmetries cannot be exploited.

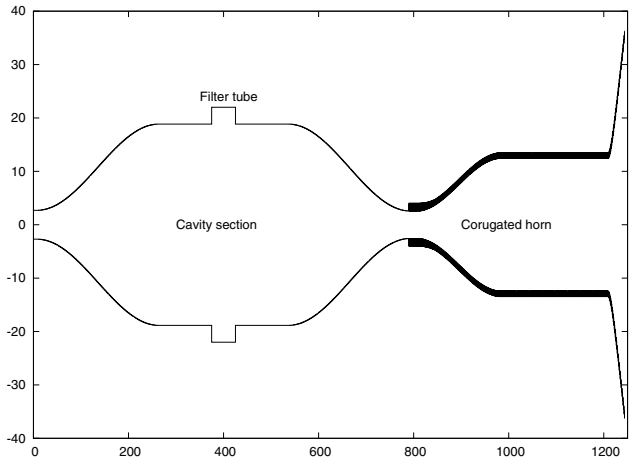

Fig. 2: Profile of the W band horn with smooth coupling sections and corrugated horn for laboratory testing of simulations. Scales are in millimetres.

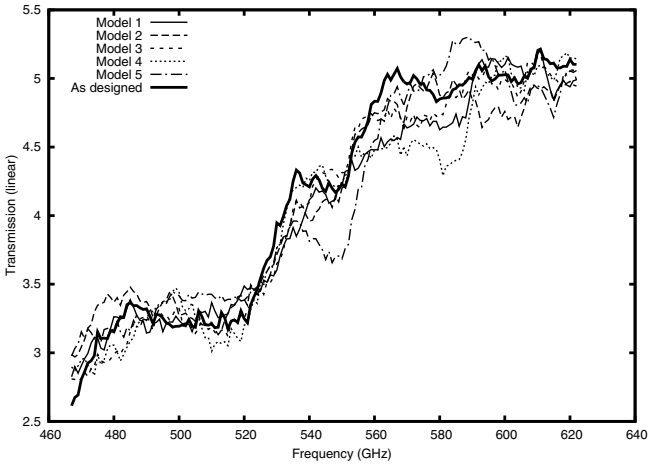

Fig. 3: 15GHz moving averages of the power transmitted through a multi-moded corrugated horn assembly of type given by equation (1). The 'as designed' curve is the simulated transmission through the ideal system. The other curves represent simulations of the same system with random manufacturing tolerances of the order $2\,\mu$m applied to the segment lengths and radii.

The presence of a cavity-like section results in trapped power and significant contributions to the field from evanescent modes. This can greatly increases the dimension of the matrices required to give an adequate model of the symmetric section $T_2^R \circ W_2 \circ F \circ W_2 \circ T_2$, or any cavity-like section. It is not necessary to maintain the same model dimension throughout the assembly.

IV. The Effects of Manufacturing Tolerances

Manufacturing tolerances result in the radii and lengths of all corrugations deviating randomly from the ideal with some statistical distribution determined by the manufacturing process. As a result there can be no two identical components and the system has to be treated as a whole. Numerical simulations and measurements show that a horn without cavity-like sections is sufficiently tolerant of small manufacturing errors that beam patterns predicted by modelling the ideal horn conform closely to measurement. When cavity-like sections

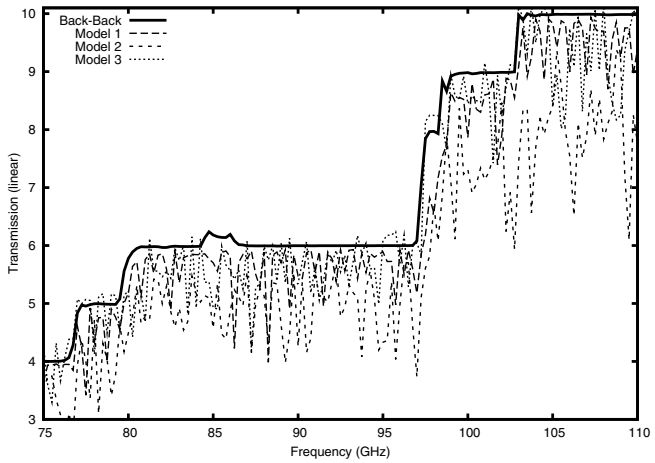

Fig. 4: Transmission trough three models of W band assemblies of the general type illustrated in Fig. 1. Model 1: as illustrated, but with the filter tube reduced to the thickness of the filter. Model 2: as illustrated. Model 3: fully corrugated assembly. The thick curve is the transmission curve through the back-to-back section of the horn with black-body illumination at the first corrugated section after the filter tube; it displays typical multi-moded power transmission. Frequency increment in model: 0.25 GHz.

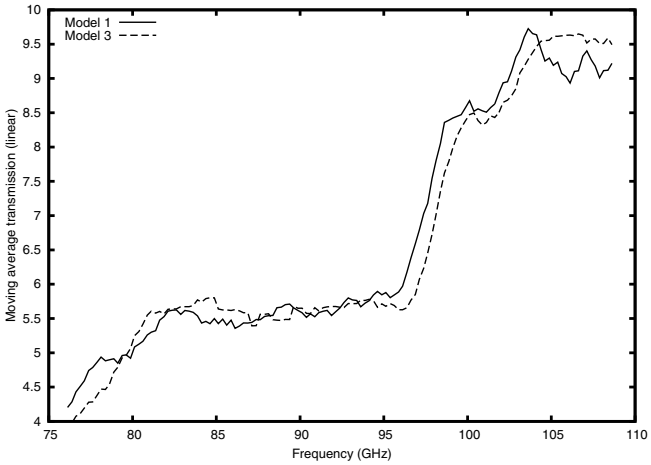

Fig. 5: 2.5 GHz (10 frequency steps) moving average power transmission models 1 and 3 in Fig. 4.

are present in the system simulations show both throughput and beam pattern varying unpredictably due to trapped power in the cavity-like sections. Beam pattern variation in a multi-moded horn is due to variation in the distribution of power between the modes (see Fig. 1). In a single moded horn there is only one azimuthal order present and the redistribution of power by a cavity-like section is only between modes of that order. Single moded horn therefore do not exhibit as severe a change in beam shape as multi-moded horns, nor such severe frequency dependent variations in transmission, except possibly in the cut-on region at the lower end of the band.

The approach we take to beam pattern prediction is stochastic modelling of large numbers of horns with appropriate randomly assigned errors on corrugation radii and lengths. Figure 3 illustrates 15 GHz moving averages in the variation in total transmission of a few moded horn assembly with cavity-like section and a 170 GHz band width centred on 545 GHz. We find the broadband beam pattern of such horns to be smooth and quite predictable, but over very narrow bands only beam shape is reasonably predictable, not throughput. Simulations indicate that the pattern of ringing is sensitive to manufacturing tolerances at the level of $\tilde{\lambda}/1000$, but this does not affect overall quality of the beam pattern. If the bolometer cavity illuminates the radiating multi-moded horn directly the system does not exhibit this acute sensitivity to manufacturing tolerances, nor the leaky cavity induced ringing.

V. Simulation results and comparison with measurement

Simulations of various systems, fully corrugated, partially corrugated and entirely smooth walled have been made. All of these systems are of the general type illustrated in figure 2. Fig. 4 shows transmission curves for three W band systems designed for laboratory testing of the numerical models. The thick black curve is the transmission through the back-to-back section assuming black-body illumination after the filter section. It exhibits typical multi-moded horn transmission with the power increasing step-wise as additional modes cut in. The wiggle at 85 GHz is due to mode leakage in azimuthal order 4 below the expected cut on at 97 GHz and indicates that the design needs to be refined.

The other three curves in Fig. 4 show the transmission through three models as described in the caption. The qualitative behaviour of the three curves is similar, and as shown in Fig. 5 the throughput of the models 1 and 3 are essentially the same. The frequency dependence of the mode structure

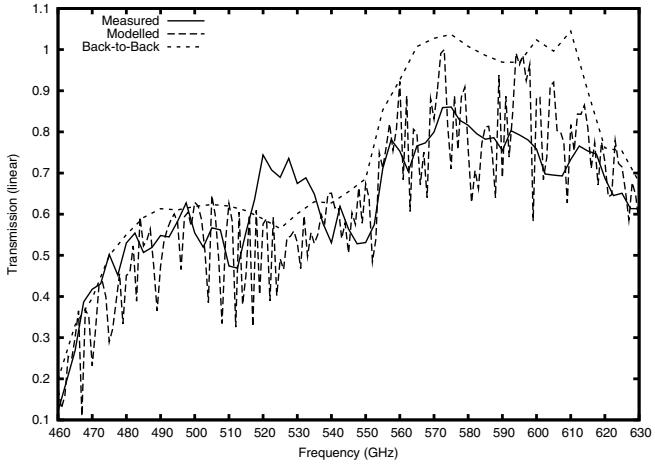

Fig. 6: Comparison of measured and modelled total power transmission for the horn assembly. The simulated transmission curve for the back-to-back section of the horn is shown for comparison. Both models are weighted for the filter stack spectral transmisivity. Fourier Transform Spectrometer measurements made by P. Ade, G. Savini, B. Maffei and R. Sudiwala, School of Physics and Astronomy, University of Cardiff.

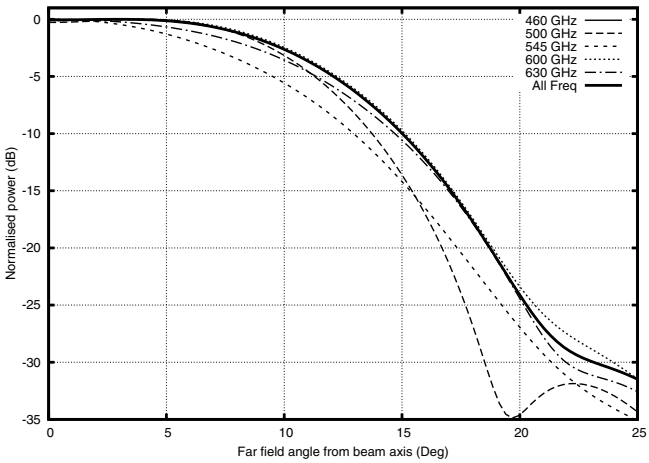

Fig. 7: Simulated far field beam pattern derived from the aperture fields, model as in Fig. 6. Five frequencies across the band and broad-band estimate based upon 64 frequencies from 460 GHz to 630 GHz.

of the aperture fields (not illustrated) is also essentially the same. When the performance uncertainties introduced by manufacturing tolerances are taken into account (see section IV) the higher manufacturing cost of the fully corrugated system suggests that the version with smooth walled coupling horns should be seriously considered: the broad band beam pattern will be essentially the same for both systems because the final pattern is determined by the corrugated radiating horn and the number of, and power distribution between, the modes in each azimuthal order at the feed into the horn from the cavity section. For both systems the number of modes are identical and the overall power in each azimuthal order are essentially the same. Care must be taken, however, in the design of the transition between smooth and corrugated sections.

Figure 6 shows the measured transmission curve for a corrugated horn assembly similar to that in Fig. 2 with $\pm 15\,\%$ band width centred on 545 GHz, a simulation of transmission through the idealised horn assembly, and a transmission envelope determined by the transmission of the back-to-back section. Both simulated systems are spectrally weighted for the transmission of the filter stack. The simulation does not account for the FTS measurement system, nor for the bolometer spectrum which is assumed to be that of a perfect blackbody. This, and the discussion of the effects of manufacturing tolerances on performance illustrates our main conclusions in section VI.

Figure 7 illustrates the broad band beam pattern over the main beam, and the beam pattern at five spot frequencies, of the 545 GHz model. All beams are individually normalised for illustration. We emphasise that all broad-band multi-moded systems show a changing beam pattern across the band due to the cutting in of additional modes as the frequency increases across the band.

VI. Conclusions

Despite the sensitivity to manufacturing tolerances, multi-moded systems of the type considered here are well suited to broad-band use such as CMB observation, but for narrow band use the manufactured horns must be carefully measured and calibrated. We have found that: (a) to get a realistic broad band beam on the sky it is necessary to simulate the complete system at at many frequencies to estimate the amount of resonance withing the system; (b) it is not possible to predict the spot frequency performance of a system because such systems are sensitive to manufacturing tolerances below the current manufacturing tolerance limits; but (c) the broad-band beam pattern is predictable for all practical purposes. Predictable because, despite the unpredictable frequency-by-frequency response of the system, the beam pattern, averaged over the pass-band of the horn frequency band does not change significantly in shape between tolerance models, though the overall transmission may vary. Indeed, even over reasonable sub-bands of around $10\,\%$ of the pass band the pattern is sufficiently predictable for practical purposes. Though they have not been discussed here, the same methods of analysis and conclusions apply to the much simpler case of single moded horn assemblies.

Acknowledgement

The authors wish to thank Peter Ade, Giorgio Savini, Bruno Maffei and Rashmi Sudiwala of the School of Physics and Astronomy, University of Cardiff, UK for providing the measurement data. We also wish to thank PRODEX and Enterprise Ireland for financial support.

References

[1] A. D. Olver, P. J. B. Clarricoats, A. A. Kishk, and L. Shafai, *Michrowave Horns and Feeds*, ser. IEEE Elecromagnetic Waves Series. IEEE Press, 1994, no. 39.

[2] P. J. B. Clarricoats and A. D. Olver, *Corrugated horns for microwave antennas*, ser. IEE Electromagnetic Waves Series. Peter Peregrinus Ltd., 1984, no. 18.

[3] J. A. Murphy, R. Colgan, C. O'Sullivan, B. Maffei, and P. Ade, "Radiation patterns of multi-moded corrugated horns for far-ir space applications," *Infrared Physics and Technology*, vol. 41, pp. 515 – 528, 2001.

[4] J. A. Murphy *et al.*, "Millimeter-wave profiled corrugated horns for the QUaD Cosmic Background Polarization Experiment," *Int. J. of Infrared and Millimeter Waves*, vol. 26, no. 4, 2005.

[5] A. Benoît *et al.*, "Archeops: a high resolution, large sky coverage balloon experiment for mapping cosmic microwave background anisotropies," *Astroparticle Physics*, vol. 17, pp. 101 – 124, 2002.

[6] B. G. Keating, P. A. R. Ade, J. J. Bock, E. Hivon, W. L. Holzapfel, A. E. Lange, H. Nguyen, and K. W. Yoon, "BICEP: A large angular scale CMB polarimeter," *Proceedings of the SPIE*, vol. 4843, pp. 284 – 295, 2003.

[7] R. E. Collin, *Field Theory of Guided Waves*, 2nd ed. IEEE Press, 1991.

[8] W. H. Press, S. A. Teukolesky, W. T. Vetterling, and B. P. Flannery, *Numerical Recipies in Fortran 77*, 2nd ed. Cambridge University Press, 2001, vol. 1.

[9] B. Maffei *et al.*, "Planck pre-launch status: HFI beam expectations from the optical optimisation of the focal plane," *Astronomy and Astrophysics*, vol. Accepted for publication, 2010.